Chemical Engineering Journal 162 (2010) 466–479

Contents lists available at ScienceDirect

Chemical Engineering Journal

journal homepage: www.elsevier.com/locate/cej

Modeling of batch electrodialysis for hydrochloric acid recovery

F.S. Rohman, M.R. Othman, N. Aziz*

School of Chemical Engineering, Engineering Campus, Universiti Sains Malaysia, Seri Ampangan, 14300, Nibong Tebal, Seberang Perai Selatan, Penang, Malaysia

ARTICLE INFO

Article history:
Received 5 October 2009
Received in revised form 17 May 2010
Accepted 17 May 2010

Keywords:
Electrodialysis
Nernst–Planck based model
Simulation
ED performances
Sensitivity analysis

ABSTRACT

Electrodialysis (ED) is a feasible method for acid recovery because it has the capability of separating ionic chemicals from non-ionic chemicals in process or waste streams to achieve product purity or eliminate wastes. At the same time, it can also enrich the separated chemicals. In this work, a model based on first principle was developed in order to understand the behavior of electrodialysis process. The Nernst–Planck derived relationship was used to build the ED process model which contains a set of ordinary differential equations (ODE). A degree of freedom analysis was carried out and a unique solution with 38 unknown parameters were identified. The parameters were determined from the literature and various equations. The developed model was then simulated and the results were compared to that from previous experimental work. The accuracy of the developed model was high with 99% degree of confidence. The sensitivity analysis of various ED parameters towards its performances was also analyzed. It was found that process time and energy consumption increased when higher initial HCl concentration in the dilute and concentrate tanks, higher current density and lower V_{conc}/V_{dil} ratio were applied. However, the effect of flowrate on process time and energy consumption was found to be insignificant.

1. Introduction

The percentage of fresh fruit bunch of oil palm which is recovered as palm oil is only 21.6% (by weight), leaving the remaining as by-products, and this includes the palm kernel and solid wastes which comprise of empty fruit bunch (EFB), fiber and shell [1]. From the EFB, sugar can be produced through the hydrolysis process by using hydrochloric acid (HCl) [2]. The remaining acid from hydrolysis must be separated from the sugars in order to yield pure sugar and to reduce the processing costs by recovering and recycling the hydrochloric acid. With the conventional neutralization process, the acid is neutralized using large amount of alkali. This renders the acid unrecoverable, and the process costly, because large amount of alkali is needed for the neutralization. Here, electrodialysis is found to be a feasible technique because it not only recovers and concentrates the hydrochloric acid but also prevents unnecessary consumption of the alkali for the neutralization process [3].

Electrodialysis (ED) is an electrochemical process for the separation of ions across charged membranes from one solution to another under the influence of electrical potential difference which is used as the driving force. It is used to remove ionized substances from liquids through selectivity ion permeable membranes. In the process, the ions are selectively transported through the appropriate membrane while non-ionic and macromolecular species are rejected [4].

In a conventional electrodialysis stack, cation and anion-exchange membranes are placed alternatively between the cathode and the anode. When a potential difference is applied between both electrodes, the cations move towards the cathode and anions towards the anode. The cations migrate through the cation-exchange membranes, which have negative fixed groups, and they are retained by the anion-exchange membranes. On the other hand, the anions migrate through the anion-exchange membranes, which have positive fixed groups, and they are retained by the cation-exchange membranes. This movement produces a rise in the ions concentration in some compartments (concentrate compartments) and the decrease in the adjacent ones (dilute). Fig. 1 shows a schematic diagram of a typical ED cell arrangement consisting of a series of anion- and cation-exchange membranes (AEM and CEM).

The principal ionic transport process that is used in electrodialysis is the migration of charged species in electric fields. The electrolyte and membranes are subjected to an electric field, and a transport of current by ionic conduction is induced. In the membrane this is dominated by migration, whereas in the electrolyte solutions this transport is complemented by diffusion and convective processes. Water transport across ion-exchange membranes accompanies electrodialysis and may consist of solution transport corresponding to primary hydration of the ions and also an additional quantity. The total solution transport caused by current is generally referred to as electro-osmosis. Osmotic transport also is a natural phenomenon in electrodialysis and the osmotic

* Corresponding author. Tel.: +60 4599457; fax: +60 45941013.
E-mail addresses: chnaziz@eng.usm.my, naziz01@yahoo.co.uk (N. Aziz).

1385-8947/$ – see front matter © 2010 Elsevier B.V. All rights reserved.
doi:10.1016/j.cej.2010.05.030

Nomenclature

Symbol

a	limiting current density coefficient ($cm^{3\alpha-b-2}\ s^b\ mol^{-\alpha}$)
a_{ERS}	electrode surface area (cm^2)
a_{me}	effective membrane surface are per each cell pair (cm^2)
A_m	overall membrane surface area (cm^2)
b	limiting current density coefficient
C_{BC}	bulk concentrate concentration ($mol\ L^{-1}$)
C_{BD}	bulk dilute concentrations ($mol\ L^{-1}$)
$C_{Bf,C}$	concentration of membrane interface in concentrate compartment ($mol\ L^{-1}$)
$C_{Bf,D}$	concentration of membrane interface in dilute compartment ($mol\ L^{-1}$)
C_c^0	initial concentration of hydrochloric acid in the feed stream ($mol\ L^{-1}$)
C_c^t	final concentration of hydrochloric acid in the feed stream ($mol\ L^{-1}$)
C_{conc}^T	concentration of hydrochloric acid (HCl) in concentrate tank ($mol\ L^{-1}$)
C_{conc}	concentration of hydrochloric acid (HCl) in concentrate compartment ($mol\ L^{-1}$)
ΔC_B	difference of acid concentration in Conc (concentrate) and Dil (dilute) compartments ($mol\ L^{-1}$)
C_{dil}^T	concentration of hydrochloric acid (HCl) in dilute tank ($mol\ L^{-1}$)
C_{dil}	concentration of hydrochloric acid (HCl) in concentrate compartment ($mol\ L^{-1}$)
D	concentration diffusion coefficient of acid through membranes ($dm^2\ s^{-1}$)
D_a	diffusion coefficient of Cl^- through anion exchange membranes ($dm^2\ s^{-1}$)
D_c	diffusion coefficient of H^+ through cation exchange membranes ($dm^2\ s^{-1}$)
E_D	Donnan potential differences (V)
E_{el}	electrode potentials (V)
E_j	junction potential differences (V)
F	Faraday constant ($C\ mol^{-1}$)
h	thickness of the electrolyte solution involved (mm)
I	current (A)
j	current density ($A\ cm^{-2}$)
j_{lim}	limiting current density ($A\ cm^{-2}$)
J_i	overall ion flux ($kmol\ m^2\ s^{-1}$)
J_w	overall water flux ($kmol\ m^2\ s^{-1}$)
J_{Wd}	flux water based on different concentration ($kmol\ m^2\ s^{-1}$)
k_m	mass transfer coefficient (dimensionless)
k_p	cost of electrical power in ED stack (RM/kWh)
l	average thickness of membranes (cm)
l_a	thickness of anion exchange membrane (cm)
l_c	thickness of cation exchange membrane (cm)
L	membrane gap (mm)
L_W	membrane constant for water transport by diffusion ($cm\ s^{-1}$)
N	number of cell pair (dimensionless)
p	vector of time independent parameter
Q_{conc}^1	flowrate of concentrate solutions discharge from the concentrate tank pump ($cm^3\ s^{-1}$)
Q_{conc}^2	flowrate of concentrate solutions discharge from the concentrate compartments ($cm^3\ s^{-1}$)
Q_{dil}^1	flowrate of concentrate solutions discharge from the dilute tank pump ($cm^3\ s^{-1}$)
Q_{dil}^2	flowrate of concentrate solutions discharge from the dilute compartments ($cm^3\ s^{-1}$)
R	electrical resistance (Ω)
R_G	gas-law constant ($mol^{-1}\ K^{-1}$)
s_a	price of acid yielded (RM/mol)
t_a^-	anion transport number in the AEM (dimensionless)
t^-	cation transport number in the AEM (dimensionless)
t_C^+	cation transport number in the CEM (dimensionless)
t_C^-	anion transport number in the CEM (dimensionless)
t^+	transport number cation in solution (dimensionless)
t_f	the final time (s)
t_i	time taking measurements (s)
t_W	water transport number (dimensionless)
T	absolute temperature (K)
V	potential drop (V)
V_{comp}	volume compartment (cm^3)
V_W	molar volume of pure water ($dm^3\ mol^{-1}$)
v	linear velocity ($cm\ s^{-1}$)
w	width of membrane (cm)
W_{elec}	electrical energy consumption (Wh)
y	actual value (dimensionless)
$\hat{y}$	simulated value (dimensionless)
$\bar{y}$	mean of the y value (dimensionless)
z	ion charge (dimensionless)

Greek variables

α	limiting current density coefficient
Γ	product recovery percentage
η	current efficiency
δ	boundary layer
Λ_0	equivalent conductance at infinite dilution
Λ	molar conductivity in solution
$\theta_1, \theta_2, \theta_3$	constant value in molar conductivity
χ	electrical conductivity

Subscripts

dil	dilute
Bf,C	the membrane surfaces in C
Bf,D	the membrane surfaces in D
C	concentrate compartment
D	dilute compartments
D,c	Donnan potential of CEM
D,a	Donnan potential of AEM
fa,C	boundary layers adjacent to the AEM in the C compartment
fa,D	boundary layers adjacent to the AEM in the D compartment
fd,C	boundary layers adjacent to the CEM in the C compartment
fd,D	boundary layers adjacent to the CEM in the D compartment
ERS	electrode rinse
ja,C	junction potential of AEM in C compartment
ja,D	junction potential of AEM in D compartment
jc,C	junction potential of CEM in C compartment
Jc,D	junction potential of CEM in D compartment

Supercripts

L	lower bound

U	upper bound
T	tank
0	initial
+	cation
−	anion

transport takes places in the same direction as the ionic transport [6].

Many researchers have studied the separation of acid and sugar using electrodialysis experimentally. These experiments include separation of lactic acid from fermentation broth which contained glucose [7], recovery of propionic and acetic acid from sugar in a fermentation broth [8], recovery of acid from acid-sugar hydrolyzate [9], separation of acetic acid from unreacted glucose and other nutrients from fermentation broths [10], deacidification of sugar in synthetic cane juice [11], separation of lactic acid from glucose-acid solution [12], and recovery of hydrochloric acid from synthetic glucose–hydrochloric acid mixture [13].

Only a few studies used models to predict the behavior of the ED and these models were basically empirical in nature. The empirical model that was employed was derived from facile mathematical tool effective within the range of phenomenological dependent coefficients obtained from experimental work such as in the recovery of acid from sulfuric acid–glucose–xylose [4], enrichment of tartaric acid from glucose in the grape juice industry waste [14], enrichment of the citric acid from fermentation broth [15], and recovery of citric acid from sugar in pineapple juice solution [16]. While this approach is very simple, it fails to represent the detailed behavior of the electrodialysis process. Due to the limitations of the empirical models, there is a need to develop another model based on a first principle that can give detailed behavior of electrotransport in the ED cell, especially on the mechanism of ion transport.

In order to gain better insight of electrodialysis, the parameters that are affected by the process must be understood and distinguished. There are three main process parameters that affect the electrodialysis performance: (1) initial concentration of feed and product solution, (2) current applied and (3) flowrate. In addition, the initial volume in the dilute and concentrate tanks, to a certain extent, also affect the ED performance due to the influence of the water transport as a result of volume difference [17]. Another parameter that indicates the performance of electrodialysis stack is product recovery percentage. Product recovery percentage gives a picture of how much the product in the feed stream can be transferred into a desired product stream. In this case, the product recovery percentage also means the separation percentage. It refers to the difference in the initial and final concentration of the electrolyte solution. Other equally important parameters that affect economy of the process include current density, potential drop across the ED stack and operating time [18,19].

In this work, development and simulation of a mathematical model based on first principle to represent the behavior of an ED unit for recovering hydrochloric acid from feed solution containing hydrochloric acid, glucose and water were endeavored. The model was validated by comparing the observed results of the previous experimental work [28]. The effects of current density, initial concentration in the dilute and concentrate tanks, initial volume in the dilute and concentrate tanks and feed flowrate on product recovery percentage, energy consumption and process time were also evaluated by the model simulation.

2. Development and sensitivity analysis of first principle model

The first principle model was derived based on the Nernst–Planck equation. The degree of freedom analysis (DOF) was carried out to ensure a unique solution can be achieved. Based on the DOF analysis, the unknown parameters were identified. The data were obtained from the manufacture data sheet and various literatures.

2.1. Model for mass transport in ED

A mathematical model based on the first principle was developed to describe electrodialysis. A Nernst–Planck (NP) equation, the irreversible thermodynamic (IT) approach, was selected due to its simplicity for use as a mathematical tool to link the flux of the species through the membrane with interfacial concentrations. The NP equation contained two terms that reflect the contribution of diffusion and electro-migration in the ionic transport. However, in this study, only one diffusion coefficient per ionic species in each phase was employed in order to be able to integrate it with other equations describing water transport through the electromembranes.

In this study, two different compartments were considered in ED, i.e., feed (dilute) and product (concentrate) compartments. The ED dilute compartment consisted of hydrochloric acid, glucose and water while the concentrate compartment consisted of hydrochloric acid and water. Glucose ($C_6H_{12}O_6$) does not decompose as it has

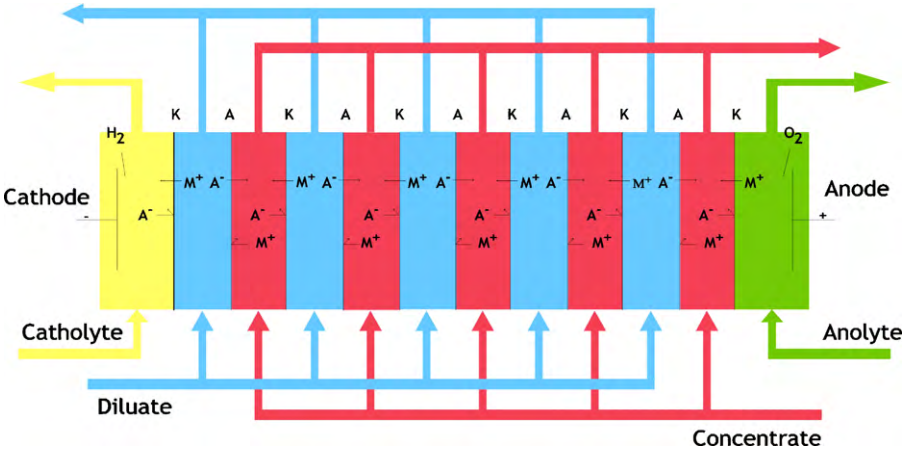

Fig. 1. Electrodialysis process with series of cation and anion exchange membranes [5].

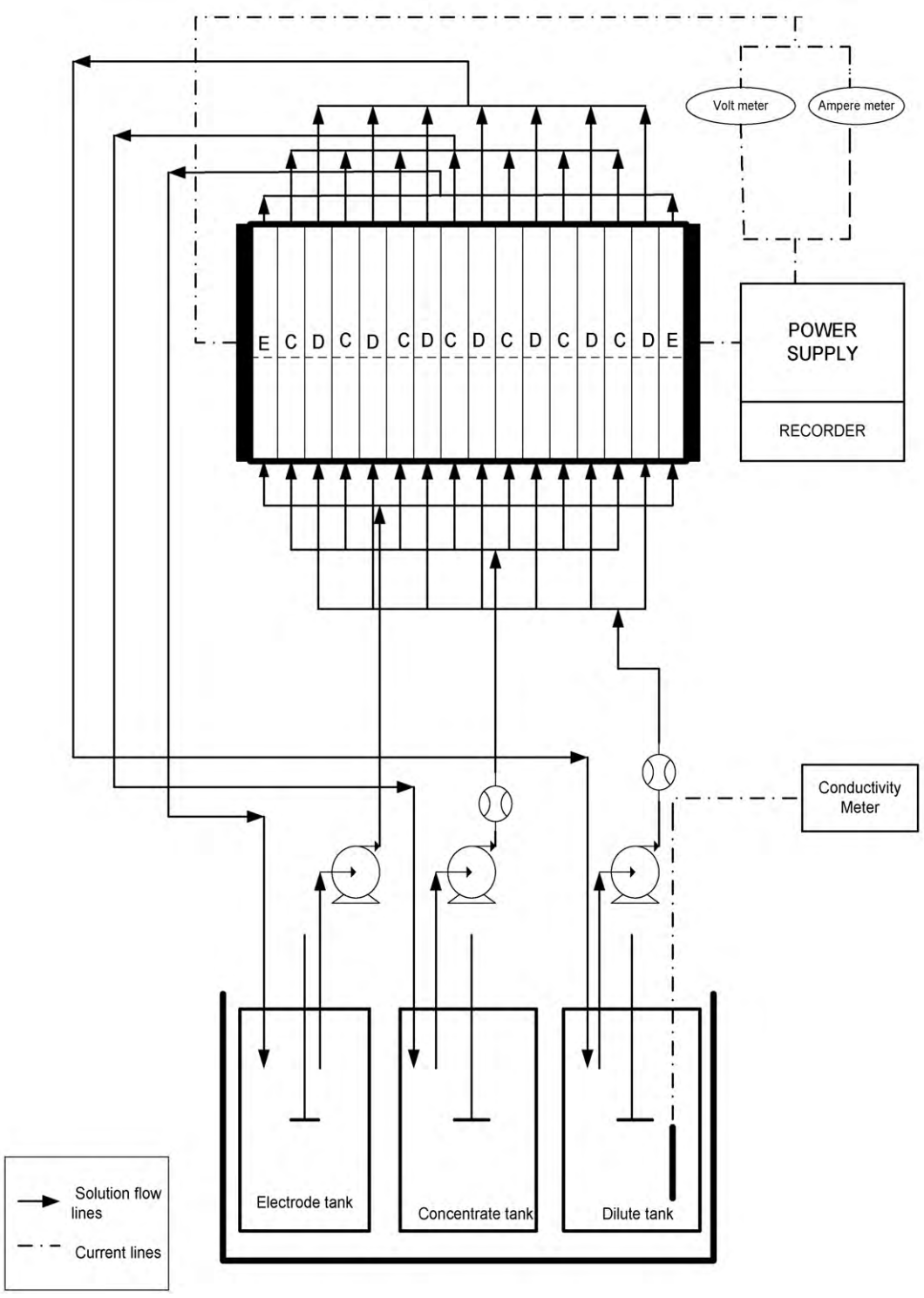

Fig. 2. Schematic diagram of ED unit.

covalent bonds which do not release free moving ions. Therefore, it remained in the feed compartment. 5 g L^{-1} concentration of glucose in dilute was used and this is based on Radzi's work [20]. The schematic diagram of the ED with batch recirculation is presented in Fig. 2.

2.1.1. The overall flux of acid

The ion flux through a generic electro-membrane can be represented as the sum of two terms; the first term is related to the applied electric field and the second term is related to ion diffusion [17]:

$$J_i = \frac{\eta j}{zF} - \frac{D_a(C_{Bf,C} - C_{Bf,D})}{l_a} - \frac{D_c(C_{Bf,C} - C_{Bf,D})}{l_c} \quad (1)$$

where z is ion charge; η is current efficiency; F is the Faraday constant; j is the current density; $C_{Bf,C}$ and $C_{Bf,D}$ are hydrochloric acid (HCl) concentrations on the surface membranes in the sides of the concentrate and dilute solutions; D_a and D_c are the diffusion

coefficients of Cl^- through the anion exchange membranes and H^+ through the cation exchange membranes respectively; and l_a and l_c are the thickness of the anion exchange membrane and the cation exchange membrane respectively. Current efficiency can be expressed by Eq. (2) [3]:

$$\eta = (t_C^+ + t_a^- - 1) - D(C_{BC} - C_{BD})\frac{F}{l(I/a_m)} \quad (2)$$

where t_C^+ and t_a^- are the cation and anion transport number in the CEM and AEM, D is the diffusion coefficient of HCl through membranes, l is the average thickness of membranes and (I/a_m) is current densities.

Based on the assumption that the boundary layers established are invariant, the concentrations of $C_{Bf,C}$ and $C_{Bf,D}$ can be calculated on the basis of the bulk concentrations, current density, and limiting current density as shown in the following equations [21]:

$$C_{Bf,C} = C_{conc}^T\left(1 + \frac{j}{j_{lim}}\right) \quad (3)$$

$$C_{Bf,D} = C_{dil}^T\left(1 - \frac{j}{j_{lim}}\right) \quad (4)$$

where C_{conc}^T, C_{dil}^T is the HCl concentration in the concentrate and dilute tanks respectively and j_{lim} is the limiting current density. j_{lim} can be described as the empirical equation related to the dilute tank concentration, C_{dil}^T, and its velocity and is shown as follows:

$$j_{lim} = aC^\alpha v^b \quad (5)$$

The a and b coefficients in Eq. (5) should be determined by measuring j_{lim} for different linear flow velocities for each specific cell design. The α coefficient should be determined by measuring j_{lim} with different dilute concentrations while $v = Q/wLN$ where w is the width of membrane, N is the number of cell pairs, Q is the flowrate of the solution and L is the membrane gap [3].

2.1.2. The overall flux of water

In the same ED cell pair, the overall water transport through the electro-membranes from the dilute to the concentrate stream can be expressed by accounting for electro-osmosis (the migration of water molecules associated with ions) and the concentration osmosis phenomenon [22].

$$J_W = \frac{t_W}{F}j + J_{Wd} \quad (6)$$

where t_W is the water transport number.

According to the Spiegler–Kedem model, J_{Wd} is proportional to the net pressure difference across the membranes. The pressure difference (ΔP) between the inter-membrane can be neglected since it is very small if compared to the overall ΔP. J_{Wd} is mainly controlled by the corresponding instantaneous osmotic pressure difference ($\Delta\pi$). Osmotic pressure difference can be assumed as proportional to the difference in HCl concentration across the membrane. Thus J_{Wd} can be expressed as:

$$J_{Wd} = L_p(\Delta\pi\sigma - \Delta P) \approx L_p\Delta\pi\sigma \approx L_W\Delta C_B \quad (7)$$

where L_W is the membrane constant for water transport by diffusion and ΔC_B is the difference of HCl concentration in the concentrate and dilute compartments [22].

2.1.3. Mass balances in an ED system

The assumptions made in developing a small scale of ED model following the Nernst idealization [17,23,24] were:

- Osmotic pressure difference was equal to the difference in HCl concentration across the membrane.
- Boundary layers adjacent to the membranes were completely static.
- The influences of the flow profile of the fluid on the model were negligible for both dilute and concentrate channels. Thus, the solution in the interior of a solution compartment was thoroughly mixed so that the concentration of the electrolyte at any point in this zone was similar.
- There was no change in the thickness of the boundary layer or the gradient along the flow channel.
- The flow dynamics were similar in all compartments.
- The distribution of pressure and current was uniform.
- Trans-membrane pressure was zero.
- There was no solution leakage in the membrane.
- Transport due to convection is ignored.

2.1.3.1. Mass balance in the ED compartments.

The mass balances for the ED stack which include the solute (HCl) and the solvent (water) in the ED compartments and in the tanks are as follows.

2.1.3.1.1. Concentrate compartment.

Water transport which occurs in the concentrate compartments can be expressed by the following equation:

$$Q_{conc}^2 = Q_{conc}^1 + J_wA_mV_w \quad (8)$$

where A_m is the overall membrane surface area, Q_{conc}^1 is the flowrate of the concentrate solutions discharge from the concentrate tank pump, Q_{conc}^2 is the flowrate of the concentrate solutions discharge from the concentrate compartments and V_W is the molar volume of pure water.

For the solute transport, the mathematical expressions are shown by the following equation:

$$V_{comp}\frac{dC_{conc}}{dt} = Q_{conc}^1C_{conc}^T - Q_{conc}^2C_{conc} + J_iA_m \quad (9)$$

where C_{conc} is HCl concentration in the concentrate compartment and V_{comp} is the volume compartment.

By replacing Eq. (8) with Eq. (9), the following equation can be obtained:

$$V_{comp}\frac{dC_{conc}}{dt} = Q_{conc}^1(C_{conc}^T - C_{conc}) + J_iA_m - J_wA_mV_wC_{conc} \quad (10)$$

2.1.3.1.2. Dilute compartment.

The equation shown below represents the mathematical expression for water transport in the dilute compartments.

$$Q_{dil}^2 = Q_{dil}^1 - J_wA_mV_w \quad (11)$$

where Q_{dil}^1 is the flowrate of the dilute solution discharge from the dilute tank pump and Q_{dil}^2 is flowrate of dilute solution discharge from the dilute compartments.

The solute transport in the dilute compartments can be expressed as:

$$V_{comp}\frac{dC_{dil}}{dt} = Q_{dil}^1C_{dil}^T - Q_{dil}^2C_{dil} - J_iA_m \quad (12)$$

where C_{dil} is the HCl concentration in dilute compartments.

By replacing Eq. (11) with Eq. (12), the following equation can be obtained:

$$V_{comp}\frac{dC_{dil}}{dt} = Q_{dil}^1(C_{dil}^T - C_{dil}) - J_iA_m + J_wA_mV_wC_{conc} \quad (13)$$

2.1.3.2. Mass balances in the tanks.

2.1.3.2.1. Concentrate tank.

Water transport in the concentrate tank is described by the following equation:

$$\frac{dV_{conc}^T}{dt} = Q_{conc}^2 - Q_{conc}^1 \quad (14)$$

By substituting Eq. (7) with Eq. (14), Eq. (15) can be formed:

$$\frac{dV_{conc}^{T}}{dt} = J_w A_m V_w \tag{15}$$

The solute transport in the concentrate tank can be expressed by the equations below:

$$\frac{d(C_{conc}^{T} V_{conc}^{T})}{dt} = Q_{conc}^{2} C_{conc} - Q_{conc}^{1} C_{conc}^{T} \tag{16}$$

Replacing Eq. (6) with Eq. (16), the following mathematical expression is derived:

$$\frac{d(C_{conc}^{T} V_{conc}^{T})}{dt} = Q_{conc}^{1}(C_{conc} - C_{conc}^{T}) + J_w A_m V_w C_{conc} \tag{17}$$

By splitting the derivative part of Eq. (17) on the left side, the following equation is formed:

$$V_{conc}^{T}\frac{dC_{conc}^{T}}{dt} + C_{conc}^{T}\frac{dV_{conc}^{T}}{dt} = Q_{conc}^{1}(C_{conc} - C_{conc}^{T}) + J_w A_m V_w C_{conc} \tag{18}$$

Substituting Eq. (15) with Eq. (18), the following complete mathematical expression can be obtained:

$$V_{conc}^{T}\frac{dC_{conc}^{T}}{dt} = Q_{conc}^{1}(C_{conc} - C_{conc}^{T}) + J_w A_m V_w (C_{conc} - C_{conc}^{T}) \tag{19}$$

2.1.3.2.2. Dilute tank. The mathematical expression related to water and solute transport in the dilute tank can be derived as shown in Eqs. (20) and (21) respectively.

$$\frac{dV_{dil}^{T}}{dt} = -J_w A_m V_w \tag{20}$$

$$V_{dil}^{T}\frac{dC_{dil}^{T}}{dt} = Q_{dil}^{1}(C_{dil} - C_{dil}^{T}) - J_w A_m V_w (C_{dil} - C_{dil}^{T}) \tag{21}$$

If $Q_{conc}^{1} = Q_{dil}^{1} = Q$, the entire mass balances derived in the concentrate and dilute compartments and in the concentrate and dilute tanks can be rearranged as Eqs. (22)–(27).

$$\frac{d(C_{conc})}{dt} = \frac{Q(C_{conc}^{T} - C_{conc}) + \left(((t_c^{+} + t_a^{-} - 1) - D(C_{conc}^{T} - C_{dil}^{T})F/jl)j - (D_a(C_{Bf,C} - C_{Bf,D}))/l_a\right) NA_m}{NV_{comp}} + \frac{(-(D_c(C_{Bf,C} - C_{Bf,D}))/l_c)NA_m - C_{conc}^{T}\left((t_W/F)j + L_W(C_{conc}^{T} - C_{dil}^{T})\right) NA_M V_W}{NV_{comp}} \tag{22}$$

$$\frac{d(C_{dil})}{dt} = \frac{Q(C_{dil}^{T} - C_{dil}) - \left(((t_c^{+} + t_a^{-} - 1) - D(C_{conc}^{T} - C_{dil}^{T})F/jl)j/F - (D_a(C_{Bf,C} - C_{Bf,D})/l_a\right) NA_m}{NV_{comp}} + \frac{(+D_c(C_{Bf,C} - C_{Bf,D})/l_c)NA_m - C_{conc}^{T}\left(-(t_W/F)j - L_W(C_{conc}^{T} - C_{dil}^{T})\right) NA_M V_W}{NV_{comp}} \tag{23}$$

$$\frac{d(C_{conc}^{T})}{dt} = \frac{Q(C_{conc} - C_{conc}^{T}) + ((t_W j/F) + (L_W(C_{conc}^{T} - C_{dil}^{T})))(C_{conc} - C_{conc}^{T})NA_M V_W}{V_{conc}^{T}} \tag{24}$$

$$\frac{d(C_{dil}^{T})}{dt} = \frac{Q(C_{dil} - C_{dil}^{T}) - (t_W j/F) + (L_W(C_{conc}^{T} - C_{dil}^{T}))(C_{dil} - C_{dil}^{T})NA_M V_W}{V_{dil}^{T}} \tag{25}$$

$$\frac{dV_{conc}^{T}}{dt} = \left(\frac{t_W}{F}j + L_W(C_{conc}^{T} - C_{dil}^{T})\right) NA_M V_W \tag{26}$$

$$\frac{dV_{dil}^{T}}{dt} = \left(-\frac{t_W}{F}j - L_W(C_{conc}^{T} - C_{dil}^{T})\right) NA_M V_W \tag{27}$$

2.1.4. Overall potential drop, resistances and energy consumption across an ED stack

The overall potential drop across an ED stack can be written as Eq. (28) [22].

$$E - E_{el} + (E_j + E_D)N = RI \tag{28}$$

where I is the current flowing through the ED device; E_{el} is the electrode potentials for the anode and cathode processes; R is the overall resistance of the membranes, the bulk solutions, the boundary layers, and the electrode rinsing solutions and E_j and E_D are the overall junction and Donnan potential differences across the boundary layers and membranes pertaining to any cell respectively; N is the overall number of cells, each one composed of a couple of anionic and cationic membranes.

The junction potential difference adjacent to the AEM and CEM membranes ($E_{ja,k}$ and $E_{jc,k}$), can be expressed in Eqs. (29)–(32) [25].

$$E_{j,a}^{conc} = \frac{R_G T}{F}(t^{+} - t^{-}) \ln\left(\frac{C_{Bf,C}}{C_{conc}^{T}}\right) \tag{29}$$

$$E_{j,a}^{dil} = \frac{R_G T}{F}(t^{+} - t^{-}) \ln\left(\frac{C_{dil}^{T}}{C_{Bf,D}}\right) \tag{30}$$

$$E_{j,c}^{conc} = \frac{R_G T}{F}(t^{+} - t^{-}) \ln\left(\frac{C_{conc}^{T}}{C_{Bf,C}}\right) \tag{31}$$

$$E_{j,c}^{dil} = \frac{R_G T}{F}(t^{+} - t^{-}) \ln\left(\frac{C_{Bf,D}}{C_{dil}^{T}}\right) \tag{32}$$

where $E_{ja,k}$ and $E_{jc,k}$ are the junction potential differences for AEM and CEM; $C_{Bf,k}$ is the solute concentration at the AEM and CEM surfaces in the concentrate and dilute compartments; R_G is the gas-law constant; T is the absolute temperature and t^{-} and t^{+} are the transport numbers for the anion and the cation in the solution.

The Donnan potential differences ($E_{D,a}$ and $E_{D,c}$) in a cell pair with the presence of a couple of anionic and cationic membranes

are expressed by [25]:

$$E_{D,a} = \frac{R_G T}{F}(t_a^- - t_a^+)\ln\left(\frac{C_{Bf,D}}{C_{Bf,C}}\right) \quad (33)$$

$$E_{D,c} = \frac{R_G T}{F}(t_c^+ - t_c^-)\ln\left(\frac{C_{Bf,D}}{C_{Bf,C}}\right) \quad (34)$$

where t_C^+ and t_C^- are the cation and anion transport numbers in the CEM and t_C^- and t_a^+ are the anion and cation transport numbers in the CEM and AEM.

The overall electric resistance of the ED stack can be expressed as follows [22]:

$$R = (R_c + R_{fc,D} + R_D + R_{fa,D} + R_a + R_{fa,C} + R_C + R_{fc,C})N + 2R_{ERS} \quad (35)$$

where $R_{fa,k}$ and $R_{fc,k}$ are the resistances of the boundary layers adjacent to the AEM and CEM membranes in the generic kth compartment; R_c and R_a, R_C and R_D, and R_{ERS} are the resistances of the cationic and anionic membranes, the bulk solution in the concentrate and dilute compartments, and the electrode rinsing solution respectively.

Except for the membrane resistances, any other generic kth ohmic resistance can be determined by applying the second Ohm's law [26]. The resistances mentioned above can be expressed mathematically with the following equations [22]:

$$R_{fa,C} = \frac{2DF}{ja_{me}\Lambda_{0,conc}(t_c^+ - t^+)} \times \ln\left[\left(\frac{\Lambda_{0,conc} + \theta_1\sqrt{C_{conc}^T}}{\Lambda_{0,conc} + \theta_1\sqrt{C_{Bf,C}}}\right)\left(\frac{\sqrt{C_{Bf,C}}}{\sqrt{C_{conc}^T}}\right)\right] \quad (36)$$

$$R_{fa,D} = \frac{2DF}{ja_{me}\Lambda_{0dil}(t_c^+ - t^+)} \times \ln\left[\left(\frac{\Lambda_{0,dil} + \theta_2\sqrt{C_{Bf,D}}}{\Lambda_{0,dil} + \theta_2\sqrt{C_{dil}^T}}\right)\left(\frac{\sqrt{C_{dil}^T}}{\sqrt{C_{Bf,D}}}\right)\right] \quad (37)$$

$$R_{fc,D} = \frac{2DF}{ja_{me}\Lambda_{0,dil}(t_a^- - t^-)} \times \ln\left[\left(\frac{\Lambda_{0,dil} + \theta_2\sqrt{C_{Bf,D}}}{\Lambda_{0,dil} + \theta_2\sqrt{C_{dil}^T}}\right)\left(\frac{\sqrt{C_{dil}^T}}{\sqrt{C_{Bf,D}}}\right)\right] \quad (38)$$

$$R_{fc,C} = \frac{2DF}{ja_{me}\Lambda_{0,conc}(t_a^- - t^-)} \times \ln\left[\left(\frac{\Lambda_{0,conc} + \theta_1\sqrt{C_{conc}^T}}{\Lambda_{0,conc} + \theta_1\sqrt{C_{Bf,C}}}\right)\left(\frac{\sqrt{C_{Bf,C}}}{\sqrt{C_{conc}^T}}\right)\right] \quad (39)$$

$$R_C = \frac{h}{a_{me}C_{conc}^T\Lambda_{conc}} \quad (40)$$

$$R_D = \frac{h}{a_{me}C_{dil}^T\Lambda_{dil}} \quad (41)$$

$$R_{ERS} = \frac{h_{ERS}}{a_{ERS}C_{ERS}\Lambda_{ERS}} \quad (42)$$

where a_{me} and a_{ERS} are the effective membrane and electrode surface areas involved in the ion flow pattern; h is the thickness of the electrolyte solution involved; Λ_0 is the equivalent conductance at infinite dilution; Λ_{ERS} is the molar conductivity of the electrode rinse solution and θ_1, θ_2 are constant values.

The molar conductivities of each compartment are calculated with the Kohlrausch equation, if the temperature and HCl concentration are known [27].

$$\Lambda_{conc} = \Lambda_{0,conc} + \theta_1\sqrt{C_{conc}^T} \quad (43)$$

$$\Lambda_{dil} = \Lambda_{0,dil} + \theta_2\sqrt{C_{dil}^T} \quad (44)$$

$$\Lambda_{ERS} = \Lambda_{0,ERS} + \theta_3\sqrt{C_{ERS}} \quad (45)$$

where $\theta_1, \theta_2, \theta_3$ are the constant values.

The energy considered in this study is the electrical energy required to transfer ions from the dilute solution to the concentrate while the energy pumps which flow in the solution is neglected. This is because the pressure drop inside the ED stack for the laboratory scale is quite small [19]. Electrical energy consumption in this ED process is calculated with the following expression:

Electrical energy consumption (Ws):

$$W_{elec} = \int_0^{tf}\left[(ja_{me})^2R + (E_{el} - (E_j + E_D)N)ja_{me}\right]\,dt \quad (46)$$

2.2. Degree of freedom analysis

The degree of freedom (DOF) analysis is conducted to ensure the equations representing the ED process can be solved. In other words, the output variables, typically the variables on the left side of the equations, can be solved in terms of the input variables on the right side of the equation. In order to have a unique solution, the number of unknown variables must equal the number of independent model equations.

For the ED system under consideration, the following information can be extracted:

- Parameter of constant values:

  $h_{ERS}, C_{ERS}, h, a_{me}, t^+, t^-, F, R_G, T, l, A_M, l_a, l_c, V_W, V_{comp}, N, w, L, a, b, \alpha, D_a, D_c, t_a^-, z, R_a, R_c$

- (27 known parameters—values taken from the literature)

  $\Lambda_{0,ERS}, \theta_2, , \theta_1, \theta_3, \Lambda_{0,conc}, \Lambda_{0,dil}, t_c^+, D, t_w, L_W, E_{el}$

- (11 unknown parameters—to be determined by using various equations)
- Variables whose values can be externally fixed (Forced variable): j, Q
- Remaining variables: C_{conc}^T, C_{dil}^T, C_{conc}, C_{dil}, V_{conc}, V_{dil}, W_{elec}, and E.
- Number of equations: eight (Eqs. (22)–(27), (28), and (46)).

The parameter of the constant values comprised of the known and determined parameters. The known parameters as tabulated in Table 1 were depicted from the manufacture data sheet and literatures. The determined parameters would be calculated using Eqs. (2), (5), (28) and (35). The DOF analysis calculation can be seen with the following expressions:

- DOF = number of variables – number of equations
- DOF = 8 – 8
- DOF = 0 (unique solution)

2.3. Determination of determined parameters

As mentioned earlier, there were 11 parameters which needed to be determined by using various equations as they were not available in the literature. Those parameters were: the equivalent

Table 1
List of parameters taken from the literature.

No.	Parameters	Value (unit)	Reference
1	a_{me}, membrane surface area	40 cm^2	[28]
2	A_m, the overall membrane surface area	200 cm^2	[28]
3	l the average thickness of membranes	0.145 mm	[28]
4	w is the width of membrane	5 cm	[28]
5	D_a the diffusion coefficient of Cl^- through A.R.A. membranes	5×10^{-9} dm^2 s^{-1}	[29]
6	l_a thickness of A.R.A. membrane	0.16 mm	[28]
7	L is the membrane gap	0.5 mm	[28]
8	R_a resistance of the A.R.A. membrane	0.048 Ω	[29]
9	t_a^- anion transport number in the A.R.A. membrane	For 0.5 M = 0.94 1 M = 0.87 2 M = 0.82 3 M = 0.66 4 M = 0.55 5 M = 0.48 6 M = 0.41	[29]
10	D_c diffusion coefficient of H^+ through C.M.V. membranes	4.9×10^{-9} dm^2 s^{-1}	[30]
11	l_c thickness of C.M.V. membrane	0.13 mm	[28]
12	R_c resistance of the C.M.V. membrane	0.0075 Ω	[3]
13	h thickness of cell	0.5 mm	[28]
14	h_{ERS} thickness of electrode chamber	2.5 mm	[28]
15	N number of ED cell	5	[28]
16	V_{comp} volume compartment	2 mL	[28]
17	a coefficient of limiting current	10 $cm^{3\alpha-b-2}$ s^b $mol^{-\alpha}$	[3]
18	b coefficient of limiting current	0.78	[3]
19	α coefficient of limiting current	0.8	[3]
20	C_{ERS} electrode rinse concentration	0.5 M	[29]
21	t^- transport number for anion in solution	0.83	[27]
22	t^+ transport number for anion in solution	0.17	[28]
23	F the Faraday constant	96485 C mol^{-1}	[27]
24	R_G gas-law constant	8.314 J mol^{-1} K^{-1}	[27]
25	T absolute temperature	303 K	[28]
26	V_W, molar volume of pure water	18×10^{-3} dm^3 mol^{-1}	[27]
27	z ion charge	1	[27]

conductance at infinite dilution for the concentrate, dilute and electrode rinse solution, $\Lambda_{0,conc}$, $\Lambda_{0,dil}$, $\Lambda_{0,ERS}$; the constant value of the molar conductivity for the concentrate, dilute and electrode rinse solution, θ_1, θ_2, θ_3; the water transport number, t_W; cation transport number in the CEM, t_C^+; electrode potentials, E_{el}; the membrane constant for water transport by diffusion, L_W, and the diffusion coefficient of HCl through the membranes, D.

2.3.1. Determination of t_C^+ and D

To determine t_C^+ and D, the correlation of current efficiency, η, Eq. (2) was used. η is related to the number of moles of an electrolyte transported from the dilute to the concentrate across the ion exchange membrane. The migration of the electrolyte was caused by the passage of electrical charges which was expressed in Faraday. As a result, the amount of ions transferred can be evaluated by measuring the changes in the concentration of HCl ions in the concentrate tank. Under constant current conditions, η at each $C^T{}_{conc}$ could be defined by Eq. (47).

$$\eta = \frac{(n_{conc}(t) - n_{conc}(0))F}{It} \tag{47}$$

where $n_{conc}(0)$, $n_{conc}(t)$ is the number of HCl moles in the concentrate tank initial and at time, t, respectively.

Figs. 3 and 4 show the HCl concentration profiles and concentrate volume profiles as a function of time in the concentrate tank for different current densities ($C_{dil}^T = 1$ M), respectively. By submitting some of the actual data from Figs. 3 and 4 in Eq. (47), η can be obtained. The data between the calculated η and $(C_{BC} - C_{BD})(F/l(I/a_m))$ for various conditions was plotted. Then the values of D and $(t_c^+ + t_a^- - 1)$ were obtained from the slope and the intercept of those related equations.

2.3.2. Determination of L_W

The water transport trend from dilute to concentrate can be expressed in the form of Eq. (48) as shown

$$V_{conc}^T(t) = V_{conc}^T(0) + \Delta V_{conc}^T \tag{48}$$

where $V_{conc}^T(t)$ is the volume solution in the concentrate tank at time t; $V_{conc}^T(0)$ is the initial volume solution in the concentrate tank, and ΔV_{conc}^T is the volume of water transported from dilute to concentrate.

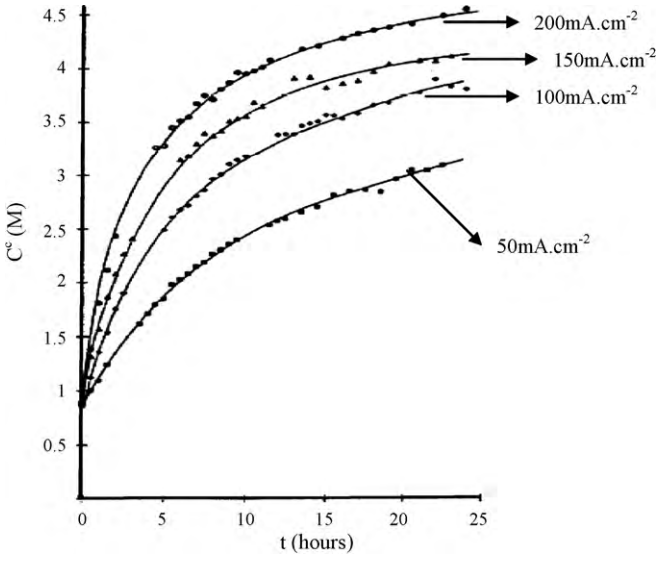

Fig. 3. HCl concentration profiles in the concentrate tank for different current densities. $C_{dil}^T(0) = 1$ M [28].

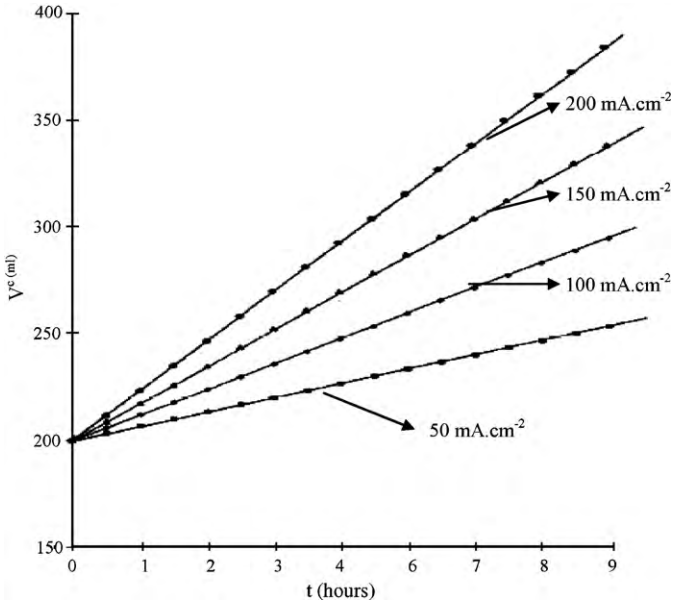

Fig. 4. Concentrate volume profiles for different current densities. $C^T_{dil}(0) = 1$ M [28].

In Fig. 4, all the lines have a similar intercept point at the y-axis. It was convenient to compare these lines under a similar initial condition. A first-order polynomial linear equation, $y = mx + c$, could be written as shown in Eq. (49):

$$V^T_{conc}(t) - V^T_{conc}(0) = a't \tag{49}$$

Rearrange and differentiate Eq. (48) to obtain Eq. (49).

$$\frac{d(V^T_{conc}(t) - V^T_{conc}(0))}{dt} = a' \tag{50}$$

While $\frac{dV^T_{conc}}{dt} = b'j$; then the summation with Eq. (50) becomes Eq. (51):

$$\frac{dV^T_{conc}}{dt} = c + dj \tag{51}$$

where $c = (a'/2)$, $d = (b'/2)$ and dV^T_{conc}/dt is the slopes of the variation of volume of concentrate with time which can be obtain from the data in Fig. 4.

Eq. (51) reveals that water transport is the sum of two effects, a flux of water proportional to the flux of charge, d and electrically silent c. Furthermore, c is equivalent to the membrane constant for water transport by diffusion, L_W, which can be obtained from the intercept of plot dV/dt versus j.

2.3.3. Determination of t_W

To determine t_W, the water transport number, the instantaneous water mole in concentrate compartments must be determined by using Eq. (52) [22]:

$$\frac{d(n_{WC})}{dt} = J_W A_M \tag{52}$$

where $n_{WC} = V^T_{conc}/V_W$ is the number of water moles in the concentrate tank and J_W is the water flux which is determined by using Eq. (5).

Eq. (52) can be integrated thus yielding:

$$\Delta n_{WC} = \int_0^t J_W A_M dt' \tag{53}$$

By replacing Eqs. (5) and (6), into Eq. (53) and operating at constant current density, the following equations can be derived:

$$\Delta n_{WC} = \frac{t_W}{F} j A_M t + L_W A_M \int_0^t \Delta C_B dt' \tag{54}$$

$$\Delta n_{WC} = n_F t_W + L_W A_M \int_0^t \Delta C_B dt' \tag{55}$$

where n_F ($=jA_m t/F$) is the theoretical equivalent mass transported according to Faraday's law. $\int_0^t \Delta C_B dt'$ can be approximated as $\Delta C_{Bint} t$ which is expressed as Eq. (56) [22]:

$$\Delta C_{Bint} = \Delta C_{B0} + \frac{\Delta C_{Bf} - \Delta C_{B0}}{t_f} t \tag{56}$$

Eq. (56) is simply a straight line passing through the points (0, ΔC_{B0}) and (t_f, ΔC_{Bf}) where ΔC_{Bf} is the difference in solute concentrations ($C_{conc} - C_{Dil}$) in the concentrate and dilute compartments at the end of the process, ΔC_{B0} is the difference in solute concentrations ($C_{Conc} - C_{Dil}$) in the concentrate and dilute compartments at the beginning of the process and t_f is the time instant at which the process is terminated (at the end of the process). By replacing Eq. (56) with Eq. (55), the following equation can be derived:

$$\Delta n_{WC} = t_W n_F + L_w A_M \left(\Delta C_{B0} t + \frac{\Delta C_{Bf} - \Delta C_{B0}}{t_f} t^2 \right) \tag{57}$$

Then, it is possible to determine the water transport number, t_W, as slope which resulted from the Δn_{WC} to n_F correlation.

2.3.4. Determination of E_{el}

If the V versus I plot in the ohmic region was independent of superficial velocity in any compartment, this would be an indirect confirmation of negligible polarization effects. By neglecting the contribution of all terms (resistances and potential differences) pertaining to the boundary layers adjacent to the electro-membranes and expressing any membrane resistance in terms of the membrane surface resistance R_m, the overall potential drop across an ED stack consisting of only anion or cation-exchange membranes can be derived from Eqs. (28) and (35) as:

$$E = E_{el} + \left[\frac{r_m}{a_{me}} N_m + R_b (N_m - 1) + 2R_{ERS} \right] I \tag{58}$$

where R_b is the resistance of the bulk solution and N_m is the overall number of AEM or CEM membranes used.

For a current smaller than one half to three fourth of the limiting current density, the voltage–current curves are practically independent of feed flow rate for any solute concentration. This resulted in an overall resistance of the ED stack (R) which is almost constant and unaffected by concentration polarization. By correlating E against I from Fig. 5, via the least squares method, as a function of concentration and velocity, it is possible to determine the electrode potential accurately.

2.3.5. Determination of $\Lambda_{0,conc}$, $\Lambda_{0,dil}$, $\Lambda_{0,ERS}$, θ_1, θ_2, θ_3

To calculate the molar conductivity of the dilute, concentrate and electrode rinse solutions (ERS), the electrical conductivity of the solutions has to be measured. By dividing electrical conductivity (χ) into solution concentration (C_B), the molar conductivity of the solution can be obtained. This correlation could be expressed by Eq. (59):

$$\Lambda = \frac{\chi}{C_B} \tag{59}$$

The experimental data of molar conductivity versus the square root of C_B is plotted. Kohlrausch limiting law is generally regarded as inadequate to describe the variation of equivalent conductivity with concentration; such a law was empirically expanded in the

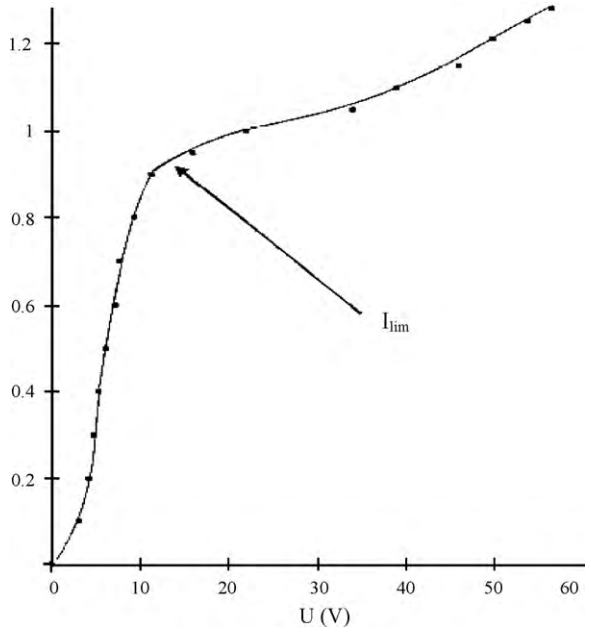

Fig. 5. Current–voltage response of the electrodialysis cell for determining the value of the limiting current [28].

powers of $\sqrt{C_B}$, that is $\sqrt{C_B}$, C_B, and ${C_B}^{3/2}$, to extrapolate the true limiting conductivity using the least squares method, thus yielding the intercept value that is the equivalent conductance in the infinitive solution (Λ_0).

2.4. Comparison and sensitivity analysis

The developed model is compared with the actual data from the literature to ensure the model proposed is reliable. Its accuracy is indicated by R^2 value. To have a better control of the ED operation, the understanding on the influence of various ED parameters to its performance is important. Due to this, a sensitivity analysis study is required.

2.4.1. Comparison of simulations result and literature

In this task, the simulated results were compared with those in the literature. In this study, Lindheimer et al.'s (1993) work was chosen as the main reference [28]. The effect of glucose on ED was neglected and only HCl transport is highlighted. Lindheimer et al. used a laboratory electrodialysis cell with the specifications as shown in Table 2.

A computer code for the model proposed was developed and solved using the ODE solver in MATLAB® version 2006b. The computer processor unit (CPU) applied is Intel Pentium 4 with capacity 3.06 GHz and 960 MB of RAM. The comparison between experimental data (represented by dotted symbol) and simulated results (represented by line) from this work is depicted in Fig. 3.

Table 2
ED specifications for Lindheimer et al.'s work.

ED specification	Value
Anion exchange membrane: A.R.A. membrane produced by Morgane	5 pieces
Cation exchange membrane: Celemion C.M.V., produced by Asahi-Glass	6 pieces
Spacers	10 pieces
DC generator: Fontaine Electronique 60 200	60 V to 20 A
Velocity of the solution	5.8 cm s^{-1}
A_M working area of the membranes	40 cm^2
V^T_{conc} initial volume solution in concentrate tank	200 mL
V^T_{dil} initial volume in dilute tank	5 L

R^2 value was used as a performance indicator. Higher R^2 values signifies that the model fitted better with the data.

$$R^2 = 1 - \frac{SSE}{SS_{yy}} \tag{60}$$

where

$$SSE = \sum \left(y - \hat{y}\right)^2 \tag{61}$$

$$SS_{yy} = \sum (y - \bar{y})^2 \tag{62}$$

y is the actual value, $\hat{y}$ is the simulated value of y and $\bar{y}$ is the mean of the y values. A perfect fit would result in an R^2 of 1, a very good fit is when R^2 is near 1 and a very poor fit is when R^2 is near 0.

2.4.2. Model sensitivity analysis

The important parameters which give significant impact to ED performances were selected based on the literature. Studies on the effect of various inputs towards selected outputs variable were carried out as detailed out below:

1. The effect of initial HCl concentration in dilute tank on process time.
2. The effect of initial HCl concentration in dilute tank on energy consumption.
3. The effect of initial HCl concentration in concentrate tank on process time.
4. The effect of initial HCl concentration in concentrate on energy consumption.
5. The effect of flowrate on process time.
6. The effect of flowrate on energy consumption.
7. The effect of current density on process time.
8. The effect of current density on energy consumption.

The effect of the initial volume of the solution in the tanks on process time and energy consumption was also analyzed. The initial volume solution in the dilute and concentrate tank influences the transport water and the ion transferred load [31]. For the same concentration applied, a higher volume tanks means more ions and water in the solution. The variation of their volume is represented in the V_{conc}/V_{dil} ratio. This analysis is useful especially for adjusting adequate ratio volume tanks.

In this study, there were 25 runs which comprise of 5 runs for each parameter. The HCl concentration of both the concentrate and dilute tank was varied in the range of 0.5–2 M. Low HCl concentrations were selected in order to prevent concentration polarization phenomenon, membrane fouling, back diffusion and low membrane permselectivity [32–37]. The V_{conc}/V_{dil} ratio used in this study was varied in 0.04, 0.5, 1, 2 and 6. The value of current density applied was varied in the range of 50–300 mA cm^{-2}. While, the flowrate used was varied between 3 and 15 cm^3 s^{-1}. The simulations of ED have target to achieve 99% degree of separation. The runs conducted in this study are tabulated in Table 3.

3. Results and discussion

3.1. Determination of t_C^+ and D

Fig. 6 shows the plot of η versus $(C_{BC} - C_{BD})(F/lj)$. Based on Eq. (2), the slope and intercept of the graph are equivalent to D and $(t_c^+ + t_a^- - 1)$ respectively. From Fig. 6, the values of slope and intercept are 2×10^{-6} cm^2 s^{-1} and 0.836 respectively. Since the value of

Table 3
Runs of various parameter for sensitivity study.

No. run	Parameter varied	Conc dilute (M)	Conc Concentrate (M)	Current density (mA cm^{-2})	Flowrate (cm^3 s^{-1})	V_{conc}/V_{dil} ratio
A1	Concentration in dilute tank	2	1	150	7.25	1
A2		1	1	150	7.25	1
A3		1.5	1	150	7.25	1
A4		0.75	1	150	7.25	1
A5		0.5	1	150	7.25	1
B1	Concentration in concentrate tank	1	2	150	7.25	1
B2		1	1	150	7.25	1
B3		1	1.5	150	7.25	1
B4		1	0.75	150	7.25	1
B5		1	0.5	150	7.25	1
C1	Current density	1	1	50	7.25	1
C2		1	1	150	7.25	1
C3		1	1	200	7.25	1
C4		1	1	300	7.25	1
C5		1	1	450	7.25	1
F1	Flow rate	1	1	150	3	1
F2		1	1	150	7.25	1
F3		1	1	150	10	1
F4		1	1	150	12.5	1
F5		1	1	150	15	1
V1	V_{conc}/V_{dil} ratio	1	1	150	7.25	0.04
V2		1	1	150	7.25	0.5
V3		1	1	150	7.25	1
V4		1	1	150	7.25	2
V5		1	1	150	7.25	6

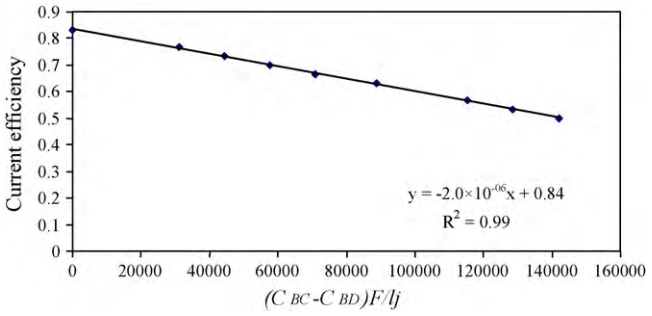

Fig. 6. Plot of η versus $(C_{BC} - C_{BD})(F/lj)$.

t_a^- is given in Table 1, the value of t_C^+ can be calculated. Thus, the value of D and t_C^+ are 2×10^{-6} cm^2 s^{-1} and 0.97 respectively.

3.2. Determination of L_W

Fig. 7 shows the plot of dV/dt versus j. L_W, the membrane constant for water transport by diffusion, can be obtained from the intercept of the graph line which is based on Eq. (51). The intercept of the graph line, which is the equivalent to L_W, is 3×10^{-5} cm s^{-1}.

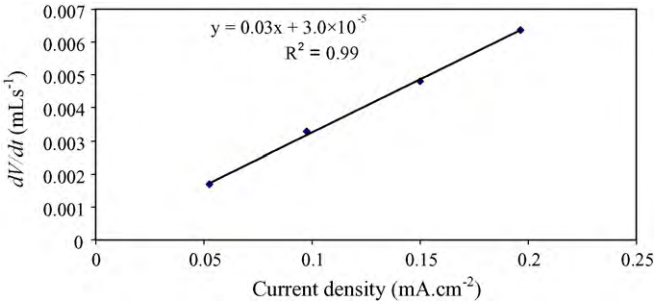

Fig. 7. Plot of dV/dt versus current density.

3.3. Determination of t_W

Fig. 8 shows the plot of net increment in water moles in the concentrate tank Δn_{WC} versus the Faraday equivalents of the solute transferred (n_F). Based on Eq. (57), the slope of the graph line is equivalent to water transport number t_W. Consequently, the t_W obtained from the figure which is the slope of the graph line, is 4.24.

3.4. Determination of E_{el}

Fig. 9 shows the plot of voltage (V) versus current (I). The electrode potential, E_{el}, can be obtained from the intercept of the graph line which is based on Eq. (58). It can be seen from Fig. 9 that the intercept of the graph line value obtained, which is the equivalent of the E_{el} value, is 2.00 V.

3.5. Determination of $\Lambda_{0,conc}$, $\Lambda_{0,dil}$, $\Lambda_{0,ERS}$, θ_1, θ_2, θ_3

Figs. 10–12 show the plot of the molar conductivity versus the square root of concentration, C_B, for concentrate, dilute and electrode rinse solutions respectively. Kohlrausch limiting law, which is empirically expanded in powers of $\sqrt{C_B}$, i.e. $\sqrt{C_B}$, C_B, and $C_B{}^{3/2}$, is used to determine $\Lambda_{0,conc}$, $\Lambda_{0,dil}$, $\Lambda_{0,ERS}$ and θ_1, θ_2, θ_3. From the

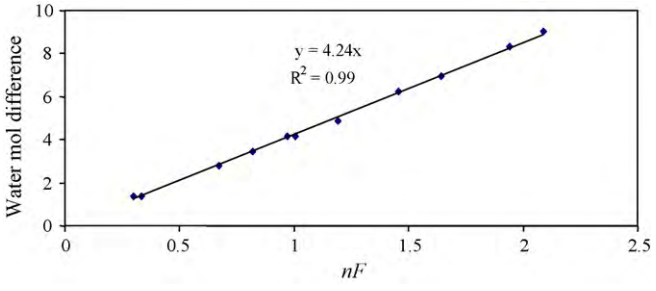

Fig. 8. Net increment in water moles in concentrate tank versus the Faraday equivalents of solute transferred (n_F).

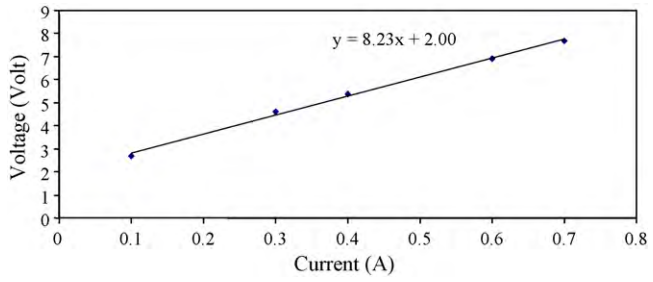

Fig. 9. Plot of voltage (V) versus current (A).

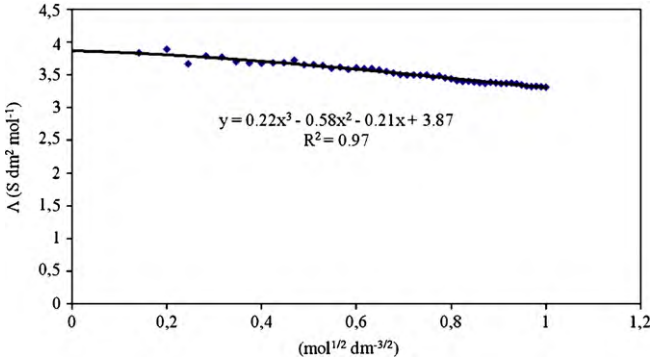

Fig. 10. Plot of Λ versus $\sqrt{C_B}$ for concentrate solution.

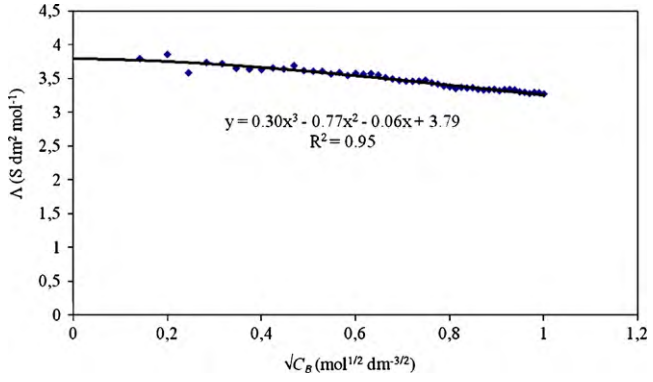

Fig. 11. Plot of Λ versus $\sqrt{C_B}$ for dilute solution.

extrapolation of the true limiting conductivity based on Eq. (59) using the least squares method, the intercept value which is equivalent to conductance in the infinitive solution of the concentrate, dilute and electrode rinse solutions (Λ_0) can be obtained. The values of θ_1, θ_2 and θ_3 are derived from the slope of $\sqrt{C_B}$.

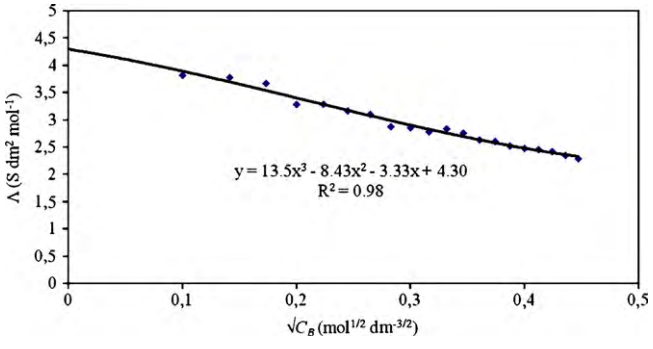

Fig. 12. Plot of Λ versus $\sqrt{C_B}$ for electrode rinse solution.

Table 4
List of unknown parameters determined by using various equations.

Determined unknown parameter	Value
Cation transport number in the CEM, t_C^+	0.97
Concentration diffusion coefficient of HCl through membranes, D	2×10^{-6} cm^2 s^{-1}
Membrane constant for water transport by diffusion, L_w	3×10^{-5} cm s^{-1}
Water transport number, t_W	4.24
Electrode potentials, E_{el}	2.00 V
Equivalent conductance for concentrate, $\Lambda_{0,conc}$	3.87 S dm^2 mol^{-1}
Constant value for concentrate in molar conductivity, θ_1	−0.21 S dm$^{7/2}$ mol$^{3/2}$
Equivalent conductance for dilute, $\Lambda_{0,dil}$	3.79 S dm^2 mol^{-1}
Constant value for dilute in molar conductivity, θ_2	−0.06 S dm$^{7/2}$ mol$^{3/2}$
Equivalent conductance for electrode rinse, $\Lambda_{0,ERS}$	4.30 S dm^2 mol^{-1}
Constant value for electrode rinse in molar conductivity, θ_3	−3.33 S dm$^{7/2}$ mol$^{3/2}$

From Figs. 10–12, the values of $\Lambda_{0,conc}$, $\Lambda_{0,dil}$, $\Lambda_{0,ERS}$ are obtained from the intercept of the graph and θ_1, θ_2, θ_3 are obtained from the slope of $\sqrt{C_B}$. Those values are listed below:

- $\Lambda_{0,conc} = 3.87$ S dm^2 mol^{-1} $\quad \theta_1 = -0.21$ S dm$^{7/2}$ mol$^{3/2}$
- $\Lambda_{0,dil} = 3.79$ S dm^2 mol^{-1} $\quad \theta_2 = -0.06$ S dm$^{7/2}$ mol$^{3/2}$
- $\Lambda_{0,ERS} = 4.30$ S dm^2 mol^{-1} $\quad \theta_3 = -3.33$ S dm$^{7/2}$ mol$^{3/2}$

All the unknown parameters that have been determined in this section are tabulated in Table 4.

3.6. ED model comparison

The model proposed is simulated using parameters from both the literature and model calculation as shown in Tables 1 and 4 respectively. The simulated results are then compared with the actual data depicted in Fig. 3.

The initial conditions of the variables involved are: $C^T_{conc}(0) = 0.85$ M, $C^T_{dil}(0) = 1$ M, $V^T_{conc}(0) = 200$ mL, $V^T_{dil}(0) = 5$ L, $Q = 7.25$ cm^3 s^{-1}. The final HCl concentration in the concentrate tank for various current density, i.e. $j = 100$, 150 and 200 mA cm^{-2}, were compared.

Fig. 13 shows the plot of the simulation results versus real data. It can be observed that the simulation results fit the actual data very well since the $R^2 \geq 99\%$ for all the cases.

3.7. Sensitivity analysis of proposed model

All the simulation results for 25 runs are tabulated in Table 5 which is contained of the process time required and energy consumed to achieve 99% degree separation.

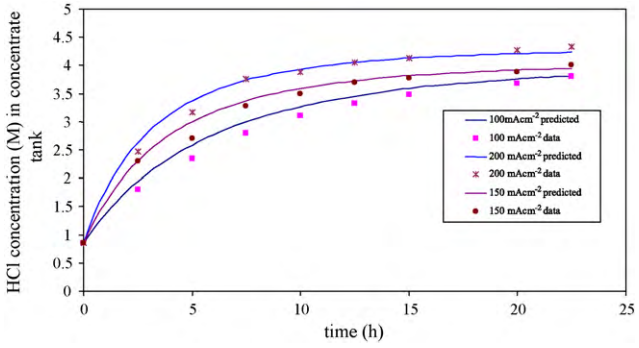

Fig. 13. Plot of C^T_{conc} versus time.

Table 5
Process time required and energy consumed from runs of various parameter.

No. run	Process time (h)	Energy consumption (Wh)
A1	23.2	624
A2	18.5	498
A3	13.1	353
A4	10.2	273
A5	6.96	187
B1	20.6	555
B2	16.1	432
B3	13.1	353
B4	12.0	324
B5	11.1	299
C1	39.4	222
C2	13.1	353
C3	9.86	419
C4	6.57	550
C5	4.39	748
F1	13.16	353.6
F2	13.14	353.2
F3	13.14	353.1
F4	13.13	353.0
F5	13.13	353.0
V1	50.1	1344
V2	24.1	648
V3	13.1	353
V4	9.06	244
V5	2.90	78

3.7.1. Effect of initial HCl concentration in dilute and concentrate tanks on process time

From the process time required for A1–A5 and B1–B5 can be seen that the increase of the initial HCl concentration in the dilute and concentrate tanks will prolong process time. This is because a higher initial HCl concentration will lead to a high amount of ions to be transferred; thereby, the time needed to separate 99% of its solution will be significantly longer. A similar trend was also observed previously [38] using ammonium chloride.

3.7.2. Effect of initial HCl concentration in dilute and concentrate tanks on energy consumption

The amount of energy consumed at different initial HCl concentrations in the dilute and concentrate tanks for run A1–A5 and B1–B5 can be seen that at a higher HCl concentration, the energy consumption required is also higher. This is because at a higher concentration, solution conductivity increased, leading to lower resistance and higher potential drops. The results were in agreement with the previous work on ED for wastewater treatment [39–41].

3.7.3. Effect of V_{conc}/V_{dil} ratio towards process time

Based on process time needed to achieve 99% degree separation for run V1–V5 was found that the process time required was longer with the decrease of the V_{conc}/V_{dil} ratio. This is because the amount of the initial solute increased significantly with a decrease of the V_{conc}/V_{dil} ratio. In addition, the low V_{conc}/V_{dil} ratio also increased the load of ions transferred from the dilute to the concentrate.

3.7.4. Effect of V_{conc}/V_{dil} ratio on energy consumption

Energy consumption obtained for run V1–V5 denotes that the lower V_{conc}/V_{dil} ratio, the higher the energy consumption. As mentioned earlier, the lower V_{conc}/V_{dil} ratio leads to a longer process time. Since current density is constant, the increase in the process time increased the energy required.

3.7.5. Effect of current density towards process time

The results of HCl removal at different current density constant flowrate and initial concentration for run C1–C5 can be observed that at a lower current density, a longer time is needed to achieve 99% degree of separation. This result is in agreement with that reported [23] for the sodium lactate recovery. The rate of ion migration through the membranes proportionally increased with current density. Thus, increasing current density obviously enhanced the ion transport through the membranes. Consequently, the process time taken was shorter.

3.7.6. Effect of current density on energy consumption

The effect of current density on energy consumption under constant flowrate and initial feed/product concentration in run C1–C5 can be observed that the higher current density applied, more energy was consumed. Energy consumption is a power function of the current density applied. In addition, the energy consumption is increased due to higher overvoltages and power losses to the solution and membrane resistance as current density was increased.

3.7.7. Effect of flowrate on process time

The effect of HCl concentration in the dilute and concentrate tanks towards process time for different flowrates for run F1–F5 indicates that a higher flowrate requires a shorter process time. However, the difference is insignificant and can be neglected.

3.7.8. Effect of flowrate on energy consumption

The energy consumption for various flowrates for run F1–F5 shows that a higher flowrate consumes less energy. However, the differences of the energy consumption for all cases are small. This is because a higher flowrate can reduce the thickness of the boundary layer. Consequently, the reduction of the thickness leads to a small energetic barrier. Therefore, the thinned layer obtained can enhance the transfer ions and thus, decrease the amount of energy consumption required.

4. Conclusions

In this study, the first principle model was developed in order to represent the transport phenomena and the electrochemical system in the ED batch process. The Nernst–Planck equation, which is the irreversible thermodynamic approach, was used to describe the ions and water transport inside the ED cell. The Henderson, Kohlrausch, Ohm and Kirchhoff equations were implemented to express the potential drops and resistances in the ED stack.

To ensure the equations representing the ED process can be solved and has a unique solution, the degree of freedom (DOF) analysis was carried out. From the analysis, 38 unknown parameters were identified. 27 of which relate to the membrane and the ED stack geometry, the transport properties of the membranes and solution, limiting current index constant and physical properties. The remaining 11 parameters were obtained using various equations.

All the models presented in this paper were able to fit the experimental data quite well and they can be employed for use and prediction of batch electrodialysis for HCl recovery.

Acknowledgement

The research grant provided by Yayasan Felda to carry out this work at Universiti Sains Malaysia is greatly acknowledged.

References

[1] Y. Basiron, Palm oil and its global supply and demand prospects, Oil Palm Industry Economic Journal 2 (1) (2002) 1–10.

[2] A. Ideris, Palm oil empty fruit bunch hydrolysis: process and optimization studies, Thesis, University of Science Malaysia, 2005.
[3] K. Urano, T. Ase, Y. Naito, Recovery of acid from wastewater by electrodialysis, Desalination 51 (1984) 213–226.
[4] T.C. Huang, R.S. Juang, Recovery of sulfuric acid with multicompartment electrodialysis, Industrial & Engineering Chemical Process Design and Development 25 (1986) 537.
[5] PCCell, Electrodialysis Unit ED 64202: Operation and Maintenance Instruction, PCCell GmBH, Germany, 1996.
[6] V.K. Indusekhar, N. Krishnaswamy, Water transport studies on interpolymer ion-exchange membranes, Desalination 52 (1985) 309–316.
[7] M. Hongo, Y. Nomura, M. Iwahara, Novel method of lactic acid production by electrodialysis fermentation, Applied and Environmental Microbiology 52 (2) (1986) 314–319.
[8] A.J. Weier, B.A. Glatz, C.E. Glatz, Recovery of propionic and acetic acids from fermentation broth by electrodialysis, Biotechnology Progress 8 (1992) 479–485.
[9] Goldstein, Method for recovering acid from an acid-sugar hydrolyzate, United *States Patent* 5,244,553 (1993).
[10] U.N. Chukwu, M. Cheryan, Electrodialysis of acetate fermentation broths, Applied Biochemistry and Biotechnology (1999) 77–79.
[11] S. Jetoo, neutralization of sugar cane juice using electrodialysis, Thesis, University of Queensland, 2000.
[12] L. Madzingaidzo, H. Danner, R. Braun, Process development and optimisation of lactic acid purification using electrodialysis, Journal of Biotechnology 96 (2002) 223–239.
[13] N.C. Radzi, Separation of hydrochloric acid and glucose using electrodialysis, Master Thesis, Universiti Sains Malaysia, 2007.
[14] L.J. Andres, F.A. Riera, R. Alvarez, Recovery and concentration by electrodialysis of tartaric acid from fruit juice industries waste waters, Journal of Chemical Technology & Biotechnology 70 (1997) 247–252.
[15] L.P. Ling, H.F. Leow, M.R. Sarmidi, Citric acid concentration by electrodialysis: ion and water transport modeling, Journal of Membrane Science 199 (2002) 59–67.
[16] M. Sairi, Deacidification of pineapple juice using electrodialysis with monopolar ion exchange membranes, Master Thesis, Universiti Teknologi Malaysia, Malaysia, 2005.
[17] V. Montiel, A. Aldaz, J.M. Ortiz, J.A. Sotoca, E. Exposito, G. Gallud, Brackish water desalination by electrodialysis: batch recirculation operation modeling, Journal of Membrane Science 252 (2005) 65–75.
[18] S.J. Parulekar, Optimal current and voltage trajectories for minimum energy consumption in batch electrodialysis, Journal of Membrane Science 148 (1998) 91–103.
[19] H.J. Lee, H. Strathmann, S.H. Moon, Determination of the limiting current density in electrodialysis desalination as an empirical function of linear velocity, Desalination 190 (2006) 43–50.
[20] N.C. Radzi, A.L. Ahmad, N. Aziz, Separation of sugars and hydrochloric acid using electrodialysis: feasibility study, in: Proceedings of the International Conference on Environment (ICENV 2006), Penang, Malaysia, 2006.
[21] V.M. Barragan, C.R. Bauza, Current–voltage curves for ion-exchange membranes: a method for determining the limiting current density, Journal of Colloid and Interface Science 205 (1998) 365–373.
[22] M. Fidaleo, M. Moresi, Optimal strategy to model the electrodialytic recovery of a strong electrolyte, Journal of Membrane Science 260 (2005) 90–111.
[23] N. Boniardi, R. Rota, G. Nano, B. Mazza, Analysis of the sodium lactate concentration process by electrodialysis, Separations Technology 6 (1996) 43–54.
[24] M. Law, T. Wen, G.S. Solt, Thickness and concentration profile of the boundary layer in electrodialysis, Desalination 109 (1997) 5–103.
[25] N. Boniardi, R. Rota, G. Nano, B. Mazza, Lactic acid production by electrodialysis. Part II. Modelling, Journal of applied electrochemistry 27 (1997) 35–145.
[26] J.S. Newman, Electrochemical Systems, Prentice Hall International Series in the Physical and Chemical Engineering Sciences, 2nd edition, 1991.
[27] J.O'M. Bockris, A.K.N. Reddy, Modern Electrochemistry, Plenum Press, 1970.
[28] A. Lindheimer, D.M. Boudet, C. Gavach, Electrodialysis of hydrochloric acid, Desalination 94 (1993) 151–165.
[29] M.B. Dumy, A. Lindheimer, C. Gavach, Transport properties of anion exchange membranes in contact with hydrochloric acid solutions. Membranes for acid recovery by electrodialysis, Journal of Membrane Science 57 (1991) 57–68.
[30] A. Heintz, E. Wiedemann, J. Ziegler, Ion exchange diffusion in electromembranes and its description using the Maxwell–Stefan formalism, Electrochimica Acta 48 (2003) 2563–2569.
[31] G.S. Luo, S. Pan, J.G. Liu, Use of the electrodialysis process to concentrate a formic acid solution, Desalination 150 (2002) 227–234.
[32] J.J. Barney, J.L. Hendrix, Regeneration of waste acid from a new ilmenite treatment process by electrodialysis, Industrial & Engineering Chemistry Product Research and Development 17 (2) (1978) 148–155.
[33] P.M. Shah, J.F. Scamehorn, Use of electrodialysis to deionize acidic wastewater streams, Industrial & Engineering Chemistry Research 26 (1987) 269–277.
[34] Khairul Faezah Md. Yunos, Electrodialysis process for recovery of citric acid using simulated medium, Universiti Teknologi Malaysia, Master Thesis, 2002.
[35] T. Mohammadi, A. Razmi, M. Sadrzadeh, Effect of operating parameters on Pb^{2+} separation from wastewater using electrodialysis, Desalination 167 (2004) 379–385.
[36] M. Sadrzadeh, T. Mohammadi, J. Ivakpour, N. Kasiri, Separation of lead ions from wastewater using electrodialysis: comparing mathematical and neural network modeling, Chemical Engineering Journal (2008).
[37] M. Sadrzadeh, T. Mohammadi, Sea water desalination using electrodialysis, Desalination 221 (2008) 440–447.
[38] S. Farrell, R.P. Hesketh, C.S. Slater, Exploring the potential of electrodialysis, Membranes in ChE Education, 2003, 52–59 [Online]. (accessed 10.11.04], Available from www.che.utexas.edu/nams/farrell.pdf.
[39] K.H. Choi, T.Y. Jeoung, Removal of zinc ions in wastewater by electrodialysis, Korean Journal of Chemical Engineering 19 (1) (2002) 107–113.
[40] A. Güvenç, B. Karabacakolu, Use of electrodialysis to remove silver ions from model solutions and wastewater, Desalination 172 (2005) 7–17.
[41] N. Kabay, O. Arar, S. Samatya, U. Yuksel, M. Yuksel, Separation of fluoride from aqueous solution by electrodialysis: effect of process parameters and other ionic species, Journal of Hazardous Materials 153 (2008) 107–113.